Bioorganic & Medicinal Chemistry Letters 20 (2010) 5217–5220

Contents lists available at ScienceDirect

Bioorganic & Medicinal Chemistry Letters

journal homepage: www.elsevier.com/locate/bmcl

X-ray crystal structure of JNK2 complexed with the p38α inhibitor BIRB796: Insights into the rational design of DFG-out binding MAP kinase inhibitors

Andreas Kuglstatter [*,†], Manjiri Ghate, Stan Tsing, Armando G. Villaseñor, David Shaw [‡], Jim W. Barnett, Michelle F. Browner [§]

Roche Palo Alto, 3431 Hillview Avenue, Palo Alto, CA 94304, USA

ARTICLE INFO

Article history:
Received 8 June 2010
Revised 28 June 2010
Accepted 30 June 2010
Available online 23 July 2010

Keywords:
JNK2
p38
BIRB796
Protein crystallography
X-ray crystal structure
DFG-out
Protein kinase
Kinase inhibitor
Structure-based drug design

ABSTRACT

JNK2 and p38α are closely related mitogen-activated protein kinases that regulate various cellular activities and are considered drug targets for inflammatory diseases. We have determined the X-ray crystal structure of the clinical phase II p38α inhibitor BIRB796 bound to its off-target JNK2. This shows for the first time a JNK subfamily member in the DFG-out conformation. The fully resolved activation loop reveals that BIRB796 inhibits JNK2 activation by stabilizing the loop in a position that does not allow its phosphorylation by upstream kinases. The structure suggests that substituents at the BIRB796 morpholino group and modifications of the *t*-butyl moiety should further increase the p38α to JNK2 potency ratio. For the design of selective DFG-out binding JNK2 inhibitors, the binding pocket of the BIRB796 tolyl group may have the best potential.

Mitogen-activated protein (MAP) kinases play key roles in the transmission of signals from cell surface receptors to transcription factors which upregulate the expression of pro-inflammatory cytokines. The MAP kinase p38α plays a key role in the biosynthesis of TNF-α, IL-1, IL-6 and IL-8, and has been found to induce the production of COX-2, MMP-1 and MMP-3.[1,2] c-Jun N-terminal kinase (JNK), also a MAP kinase, is involved in the production of phospho-c-Jun and AP-1 as well as the upregulation of MMP-1, MMP-3 and MMP-13.[3,4] Redundant and non-redundant functions of the JNK isoforms JNK1 and JNK2 in the immune system and arthritis have been described.[5] Consequently, both p38α and JNK have been targeted for the discovery of small-molecule therapeutics for inflammatory diseases.[6–8]

The diaryl urea p38α inhibitor BIRB796 (Fig. 1A, K_D = 0.16 nM) blocks TNF-α production in cell cultures and it is efficacious in both collagen-induced arthritis and endotoxin-stimulated TNF-α release animal models.[9] BIRB796 also has been shown to be a strong inhibitor of TNF-α production in lipopolysaccharide-induced endotoxemia, a model for inflammation in humans.[10] Published results of phase I[6] and phase II[11] clinical trials in Crohn's disease and rheumatoid arthritis have been summarized recently. BIRB796 also binds with high affinity to JNK2 (K_D = 4.6 nM)[12] and with lower affinity to JNK3 (K_D = 62 nM), but it shows no significant binding to JNK1.[13] In HCA2 cells, BIRB796 at least partially inhibits total activity of the JNK subfamily at concentrations higher than 1.0 μM.[14] It has been reported that the pharmacological activity of BIRB796 is mainly due to its p38α inhibitory activity.[12] To what extent the JNK2 activity of BIRB796 is responsible for the potentially drug-related adverse events observed in clinical trials, for example, infections and rashes,[15] is unclear.

The X-ray crystal structure of p38α in complex with BIRB796 revealed that this inhibitor blocks p38α signaling by stabilizing the 'DFG-out' conformation of p38α,[9] which makes it a so-called 'type II' kinase inhibitor. This conformation does not allow ATP binding to the enzyme, and it is typically associated with slow

Abbreviations: JNK, c-Jun N-terminal kinase; MAP, mitogen-activated protein.

* Corresponding author. Tel.: +1 973 235 7345; fax: +1 973 235 8622.
E-mail address: andreas.kuglstatter@roche.com (A. Kuglstatter).
† Present address: Hoffmann-La Roche, 340 Kingsland Street, Nutley, NJ 07110, USA.
‡ Present address: Genentech, Inc., 1 DNA Way, South San Francisco, CA 94080, USA.
§ Present address: F. Hoffmann-La Roche AG, 4070 Basel, Switzerland.

0960-894X/$ - see front matter © 2010 Elsevier Ltd. All rights reserved.
doi:10.1016/j.bmcl.2010.06.157

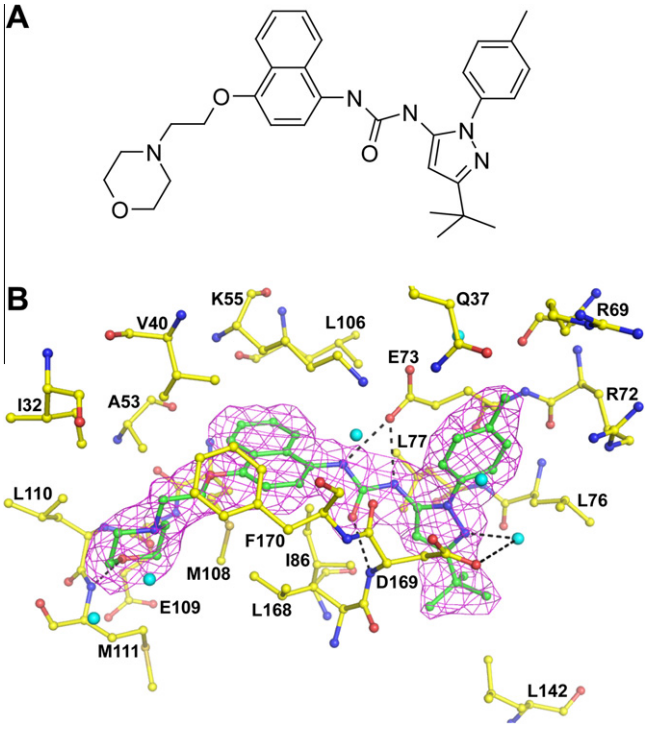

Figure 1. X-ray crystal structure of JNK2 with BIRB796 bound. (A) Structural formula of BIRB796. (B) Ball-and-stick representation of JNK2 residues (yellow) within 4 Å of BIRB796 (green). Water molecules are displayed in cyan. Protein-ligand H-bonds are indicated as black hashes. A $2F_0 - F_c$ electron density map contoured at 1σ is displayed in magenta.

binding kinetics. It has been postulated that protein kinase inhibitors that bind to the DFG-out conformation provide a better starting point for the design of highly selective inhibitors compared to 'type I' inhibitors that bind to the 'DFG-in' conformation.[16–18] Consequently, different screening methods that allow identification of DFG-out binders have recently been developed and successfully deployed for p38α.[19,20] JNK specific DFG-out inhibitors, however, have not been reported to our knowledge, and a crystal structure of JNK in the DFG-out conformation is not available in the public domain. This prompted us to determine the X-ray crystal structure of JNK2 in complex with BIRB796. This structure will facilitate the design of JNK2 selective diaryl urea inhibitors in particular and DFG-out binders in general. The structural information obtained also allows the rational design of BIRB796 analogues as p38α inhibitors with decreased JNK affinity, which may improve the therapeutic potential for this compound class.

Untagged JNK2α kinase domain comprising amino acids 1–364, the JNK3 chimera mutations D3K, C6V, S8N and Q14E, and the surface mutations K203A, E204A, K250A and K251A was over-expressed in *Escherichia coli* and purified following a protocol described previously.[21] These amino acid exchanges occur at least 12 Å away from the binding site of the BIRB796 molecule and therefore do not affect its binding to JNK2. Remarkably, the set of JNK2 surface mutations required for the co-crystallization of BIRB796 is different from that used to co-crystallize the indazole inhibitor furan-2-carboxylic acid {3-[5-(4*H*-[1,2,4]triazol-3-yl)-1*H*-indazol-3-yl]-phenyl}-amide.[21] The mutant JNK2 protein at a concentration of 10 mg/ml (25 mM HEPES (pH 7.5), 0.1 M sodium chloride, 0.01 M magnesium chloride, 5% glycerol, 1 mM TCEP, 0.02% Octyl-β-glucopyranoside) was incubated with 0.1 mM BIRB796 and 5% DMSO. The protein–ligand complex was crystallized by vapor diffusion in hanging drops at 20 °C. Protein solution (0.7 μl) was mixed with 0.7 μl of 0.1 M HEPES (pH 7.5), 0.1 M sodium chloride and 1.6 M ammonium sulfate. Crystals were transferred to a buffer containing 30% sucrose, 1.8 M ammonium sulfate, 0.1 M HEPES (pH 7.5), 0.1 M BIRB796 and 5% DMSO for cooling in liquid nitrogen. X-ray diffraction data were collected by Reciprocal Space Consulting, LLC (Oakland, California, USA) at the synchrotron beam line 9-2 of the Stanford Synchrotron Radiation Laboratory (Palo Alto, California, USA) using an ADSC Quantum 315R CCD detector. The diffraction images were processed using DENZO and the intensities were scaled using SCALEPACK[22] to 2.35 Å resolution with good statistics: completeness = 99.9% (100% in highest resolution shell), $I/\sigma(I) = 11.1$ (2.1), $R_{sym} = 8.4\%$ (56.9%), $R/R_{free} = 21.4/25.4\%$. Molecular replacement was performed with the program PHASER[23] using the crystal structure of JNK2 complexed with the indazole inhibitor furan-2-carboxylic acid {3-[5-(4*H*-[1,2,4]triazol-3-yl)-1*H*-indazol-3-yl]-phenyl}-amide (PDB accession number 3E7O)[21] as search model. The solution found was a JNK2 dimer in space group $P2_12_12_1$ ($a = 76.2$ Å, $b = 92.3$ Å, $c = 112.1$ Å). This new crystal form should allow the co-crystallization of JNK2 with DFG-out binding inhibitors in general. The model was refined against the experimental data and electron density maps were calculated using REFMAC5.[24] The electron density for BIRB796 was well defined and it could be fitted unambiguously (Fig. 1B). The structure model was built with the graphics software MOLOC[25] and illustrations of the final crystal structures were created using PYMOL (http://www.pymol.org/). Coordinates and structure factor amplitudes have been deposited to the Protein Data Bank with accession number 3NPC.

The crystal structure described in this manuscript shows how BIRB796 binds to the DFG-out conformation of JNK2 (Fig. 2). The entire activation loop (amino acids 172–188) and the adjacent DFG sequence are resolved. D169, F170 and G171 swing out and open a pocket adjacent to helix C for the *t*-butyl-pyrazole moiety of BIRB796 (amino acids 64–79). The activation loop is stacking against the Gly-rich loop (amino acids 30–42) thereby shielding BIRB796 from solvent.

The secondary structure elements around the ATP binding pocket in the crystal structure of JNK2 complexed with BIRB796 adopt conformations distinctly different from those observed for JNK2 complexed with the indazole inhibitor furan-2-carboxylic acid {3-[5-(4*H*-[1,2,4]triazol-3-yl)-1*H*-indazol-3-yl]-phenyl}-amide (Fig. 3).[21] The Gly-rich loop in the indazole-bound structure is positioned as much as 5 Å higher and away from the bound ligands than in the

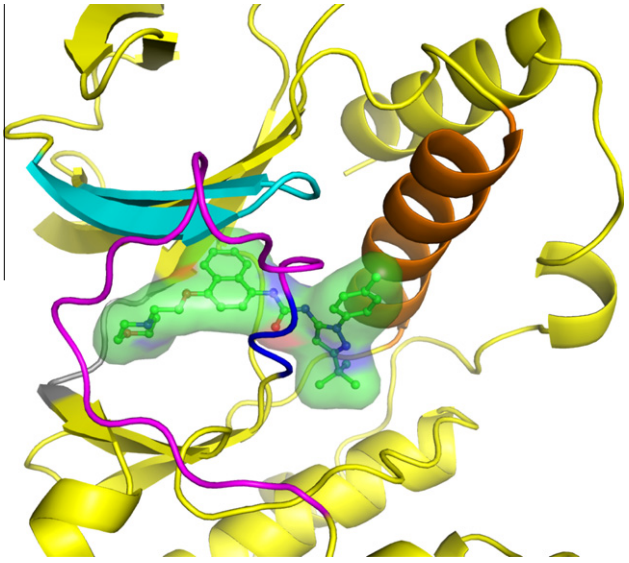

Figure 2. Ribbon representation of JNK2 around the BIRB796 binding site. Cyan: Gly-rich loop, orange: helix C, dark blue: DFG, magenta: activation loop. BIRB796 is shown in ball-and-stick and molecular surface representation in green.

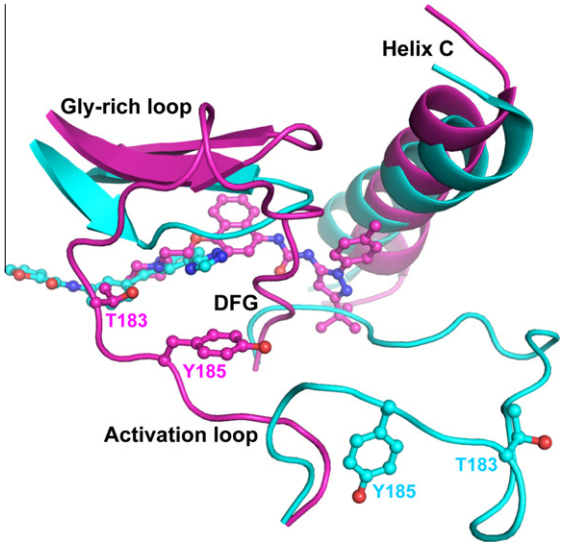

Figure 3. Superposition of the JNK2 crystal structures with the DFG-out binding BIRB796 (magenta) and a DFG-in binding indazole inhibitor (cyan, PDB accession number 3E7O) bound. The protein structure surrounding the ligand binding sites is shown in ribbon representation and the activation loop side chains that are phosphorylated upon activation are shown in ball-and-stick representation.

BIRB796-bound structure. The orientation of helix C in the two JNK2–ligand complex structures is also markedly different. The indazole inhibitor is a DFG-in binder and the activation loop in that crystal structure is stabilized by the MAP kinase insert in a position incompatible with phosphorylation by upstream kinases.[21] The MKK4 substrate Y185 is buried inside the protein and access to the MKK7 substrate T183 is sterically hindered. In the JNK2-BIRB796 crystal structure, phosphorylation of the activation loop is also hindered, but for different structural reasons. The T183 side chain is pointing into the ATP binding site preventing phosphorylation by MKK7 (Fig. 3). The side chain of Y185 is solvent exposed, yet the observed rotamer likely evades phosphorylation for steric reasons. Consequently, BIRB796 not only prevents ATP binding to the active site but it also stabilizes JNK2 in a conformation that prevents activation by upstream kinases. This provides the structural rationale for the observation that BIRB796 inhibits JNK activation in HEK293 cells.[26] In analogy, BIRB796 has been shown to prevent MKK6-dependent activation of p38α.[27]

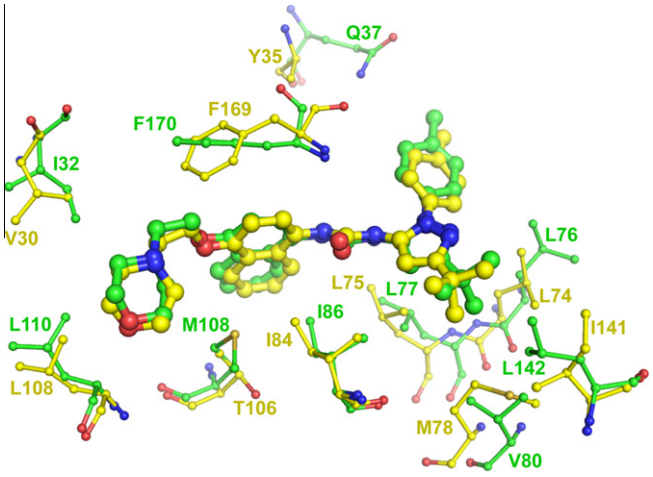

Figure 4. Superposition of the crystal structures of JNK2 (green) and p38α (yellow, PDB accession number 1KV2) with BIRB796 bound. Selected amino acids that differ between the two proteins in type or structural conformation are displayed. (The phenol moiety of the p38α residue Y35 is not part of the structure model.)

BIRB796 forms multiple hydrophobic and polar interactions with the JNK2 protein (Fig. 1B). The morpholino oxygen accepts an H-bond from the M111 backbone NH in the hinge region (amino acids 109–113) of the ATP binding site which connects the N- and C-terminal kinase lobes. In addition, the morpholino group makes lipophilic contacts with the side chains of residues I32 (Gly-rich loop), M108, L110 and M111 (all hinge region). The ethylene linker of BIRB796 interacts favorably with the side chains of I32 (Gly-rich loop) and F170 (activation loop). The BIRB796 naphthalene moiety is positioned in the so-called 'back pocket' sandwiched between the side chains of K55, I86, L106, M108, L168 and F190. The adjacent urea forms three H-bonds with the JNK2 protein: the oxygen interacts with the backbone NH of the D169 side chain (DFG) and both nitrogens interact with the side chain of the highly conserved residue E73 (helix C). The BIRB796 pyrazole moiety is positioned between the side chains of L74 (helix C) and D169 (DFG). Its orientation allows the 3-*t*-butyl group to fill a pocket formed by the side chains of Q37 (Gly-rich loop), R69, R72, E73, L76 (all helix C) and D169 (DFG). The 1-tolyl substituent occupies a highly lipophilic pocket formed by the side chains of L76, I85, I86, L142 and H149.

The superposition of the BIRB796 crystal structures bound to JNK2 and p38α[9] (Fig. 4) suggests a path towards the rational design of BIRB796 analogues that lack unwanted JNK2 activity. Firstly, small substituents at the 2-position of the BIRB796 morpholino group should be tolerated in p38α but have the potential to create steric clashes with the side chains of the JNK2 residues I32 (Gly-rich loop), L110 (hinge) and/or perhaps T183 (activation loop) (Fig. 3). The latter could potentially destabilize the phosphorylation-incompatible conformation of the activation loop observed in the JNK2-BIRB796 crystal structure. Secondly, small substituents at the morpholine 3-position could fill a small pocket bordered by the gate keeper residue T106 in p38α (Fig. 4). This pocket does not exist in JNK2 due to the larger M108 side chain. 3-Substituents also have the potential to enter a hydrophobic p38α selectivity pocket adjacent to A157[11] (V158 in JNK2). Thirdly, the difference in depth of the *t*-butyl pockets between JNK2 and p38α caused by the respective L142/I141 amino acid difference (Fig. 4) should allow the design of BIRB796 analogues with a significantly increased p38α to JNK2 potency ratio.

The superposition of the JNK2-BIRB796 and p38α-BIRB796[9] crystal structures (Fig. 4) also provides guidance for the rational design of selective JNK2 inhibitors that capitalize on the DFG-out binding conformation. Sequence and structural differences around the tip of the Gly-rich loop (Y35 in p38α, Q37 in JNK2) indicate that this region could be used to achieve differential binding between JNK2 and p38α. We propose to test this hypothesis by adding polarity to the BIRB796 tolyl group, possibly by replacing it with heterocycles or 5,6 ring systems. However, the partial lack of order in that region of the p38α-BIRB796 crystal structure makes structure-based design challenging.

In conclusion, the X-ray crystal structure of JNK2 with the p38α inhibitor BIRB796 bound demonstrates that this DFG-out binding compound inhibits JNK2 activation by stabilizing the activation loop in a conformation that is not compatible with phosphorylation by upstream kinases. We propose that modifications of the BIRB796 morpholino and *t*-butyl moieties have the potential to reduce JNK2 off-target activity. Based on the structure we suggest that the JNK2 subpocket which binds the BIRB796 tolyl moiety is a region where the design of selective DFG-out binding JNK2 inhibitors might be most effective.

References and notes

1. Schett, G.; Zwerina, J.; Firestein, G. *Ann. Rheum. Dis.* **2008**, *67*, 909.
2. Westra, J.; Limburg, P. C. *Mini-Rev. Med. Chem.* **2006**, *6*, 867.
3. Salh, B. *Expert Opin. Ther. Targets* **2007**, *11*, 1339.
4. Thalhamer, T.; McGrath, M. A.; Harnett, M. M. *Rheumatology* **2008**, *47*, 409.

5. Bogoyevitch, M. A. *BioEssays* **2006**, *28*, 923.
6. Goldstein, D. M.; Gabriel, T. *Curr. Top. Med. Chem.* **2005**, *5*, 1017.
7. Lograsso, P.; Kamenecka, T. *Mini-Rev. Med. Chem.* **2008**, *8*, 755.
8. Pettus, L. H.; Wurz, R. P. *Curr. Top. Med. Chem.* **2008**, *8*, 1452.
9. Pargellis, C.; Tong, L.; Churchill, L.; Cirillo, P. F.; Gilmore, T.; Graham, A. G.; Grob, P. M.; Hickey, E. R.; Moss, N.; Pav, S.; Regan, J. *Nat. Struct. Biol.* **2002**, *9*, 268.
10. Branger, J.; van den, B. B.; Weijer, S.; Madwed, J.; Bos, C. L.; Gupta, A.; Yong, C. L.; Polmar, S. H.; Olszyna, D. P.; Hack, C. E.; van Deventer, S. J.; Peppelenbosch, M. P.; van der, P. T. *J. Immunol.* **2002**, *168*, 4070.
11. Goldstein, D. M.; Kuglstatter, A.; Lou, Y.; Soth, M. J. *J. Med. Chem.* **2010**, *53*, 2345.
12. Gruenbaum, L. M.; Schwartz, R.; Woska, J. R., Jr.; DeLeon, R. P.; Peet, G. W.; Warren, T. C.; Capolino, A.; Mara, L.; Morelock, M. M.; Shrutkowski, A.; Jones, J. W.; Pargellis, C. A. *Biochem. Pharmacol.* **2009**, *77*, 422.
13. Fabian, M. A.; Biggs, W. H., III; Treiber, D. K.; Atteridge, C. E.; Azimioara, M. D.; Benedetti, M. G.; Carter, T. A.; Ciceri, P.; Edeen, P. T.; Floyd, M.; Ford, J. M.; Galvin, M.; Gerlach, J. L.; Grotzfeld, R. M.; Herrgard, S.; Insko, D. E.; Insko, M. A.; Lai, A. G.; Lelias, J. M.; Mehta, S. A.; Milanov, Z. V.; Velasco, A. M.; Wodicka, L. M.; Patel, H. K.; Zarrinkar, P. P.; Lockhart, D. J. *Nat. Biotechnol.* **2005**, *23*, 329.
14. Bagley, M. C.; Davis, T.; Rokicki, M. J.; Widdowson, C. S.; Kipling, D. *Future Med. Chem.* **2010**, *2*, 193.
15. Schreiber, S.; Feagan, B.; D'Haens, G.; Colombel, J. F.; Geboes, K.; Yurcov, M.; Isakov, V.; Golovenko, O.; Bernstein, C. N.; Ludwig, D.; Winter, T.; Meier, U.; Yong, C.; Steffgen, J. *Clin. Gastroenterol. Hepatol.* **2006**, *4*, 325.
16. Cowan-Jacob, S. W.; Mobitz, H.; Fabbro, D. *Curr. Opin. Cell Biol.* **2009**, *21*, 280.
17. Huse, M.; Kuriyan, J. *Cell* **2002**, *109*, 275.
18. Jacobs, M. D.; Caron, P. R.; Hare, B. J. *Proteins* **2008**, *70*, 1451.
19. Simard, J. R.; Grutter, C.; Pawar, V.; Aust, B.; Wolf, A.; Rabiller, M.; Wulfert, S.; Robubi, A.; Kluter, S.; Ottmann, C.; Rauh, D. *J. Am. Chem. Soc.* **2009**, *131*, 18478.
20. Tecle, H.; Feru, F.; Liu, H.; Kuhn, C.; Rennie, G.; Morris, M.; Shao, J.; Cheng, A. C.; Gikunju, D.; Miret, J.; Coli, R.; Xi, S. H.; Clugston, S. L.; Low, S.; Kazmirski, S.; Ding, Y. H.; Cao, Q.; Johnson, T. L.; Deshmukh, G. D.; DiNitto, J. P.; Wu, J. C.; English, J. M. *Chem. Biol. Drug Des.* **2009**, *74*, 547.
21. Shaw, D.; Wang, S. M.; Villasenor, A. G.; Tsing, S.; Walter, D.; Browner, M. F.; Barnett, J.; Kuglstatter, A. *J. Mol. Biol.* **2008**, *383*, 885.
22. Otwinowski, Z.; Minor, W. Macromolecular Crystallography, Part A. In Carter, C. W. J., Sweet, R. M., Eds.; Academic Press: New York, 1997; pp 307–326.
23. McCoy, A. J.; Grosse-Kunstleve, R. W.; Storoni, L. C.; Read, R. J. *Acta Crystallogr., Sect D* **2005**, *61*, 458.
24. Murshudov, G. N.; Vagin, A. A.; Dodson, E. J. *Acta Crystallogr., Sect D* **1997**, *53*, 240.
25. Gerber, P. R. *Biopolymers* **1992**, *32*, 1003.
26. Kuma, Y.; Sabio, G.; Bain, J.; Shpiro, N.; Marquez, R.; Cuenda, A. *J. Biol. Chem.* **2005**, *280*, 19472.
27. Sullivan, J. E.; Holdgate, G. A.; Campbell, D.; Timms, D.; Gerhardt, S.; Breed, J.; Breeze, A. L.; Bermingham, A.; Pauptit, R. A.; Norman, R. A.; Embrey, K. J.; Read, J.; VanScyoc, W. S.; Ward, W. H. *Biochemistry* **2005**, *44*, 16475.